Laser damage density measurement of optical components in the sub-picosecond regime

Martin Sozet,[1,*] Jérôme Néauport,[1] Eric Lavastre,[1] Nadja Roquin,[1] Laurent Gallais,[2] and Laurent Lamaignère[1]

[1]*Commissariat à l'Energie Atomique et aux Energies Alternatives, Centre d'Etudes Scientifiques et Techniques d'Aquitaine (CEA CESTA), CS60001, 33116 Le Barp Cedex, France*

[2]*Aix-Marseille Université, Ecole Centrale Marseille, CNRS, Institut Fresnel, Campus de St Jérôme, 13013 Marseille, France*

**Corresponding author: martin.sozet@cea.fr*

Received February 11, 2015; revised April 8, 2015; accepted April 13, 2015;
posted April 13, 2015 (Doc. ID 234218); published April 30, 2015

A rasterscan procedure adapted to the sub-picosecond regime is set to determine laser-induced damage densities as function of fluences. Density measurement is carried out on dielectric high-reflective coatings operating at 1053 nm. Whereas laser-induced damage is usually considered deterministic in this regime, damage events occur on these structures for fluences significantly lower than their intrinsic damage threshold. Scanning electron microscope observations of these "under-threshold" damage sites evidence ejections of defects, embedded in the dielectric stack. This method brings a new viewpoint for the qualification of optical components and their optimization for a high resistance in the sub-picosecond regime.

OCIS codes: (140.3330) Laser damage; (140.7090) Ultrafast lasers; (310.0310) Thin films.
http://dx.doi.org/10.1364/OL.40.002091

The past fifty years have seen several generations of high-power laser facilities devoted to laser/matter interaction and fusion study in particular. From L5, Janus, Shiva [1,2], to the National Ignition Facility (NIF) or the Laser Megajoule (LMJ) [3,4], the output power raised from gigawatts to hundreds of terawatts with the NIF using flash-pumped Nd:glass technology to produce nanosecond pulses. The chirped pulse amplification technique proposed by Strickland and Mourou in 1985 [5] paved the way for ultra-intense high-energy systems. Since then, laboratories have developed short-pulse high-power laser facilities all around the world [6]. While considering long-pulse or short-pulse high-power laser facilities, optical components performances and in particular laser damage are always factors limiting the overall system performances. A common practice is to use large beams and therefore large optical components in order to reduce the energy density. For questions of manufacturability, ease of maintenance, and cost, optics size has been limited to meter scale since the mid-90s. When larger sizes are needed, mosaic of meter-size optics can be used following the same trend as for astronomical mirrors. In this context, getting a precise knowledge of the laser optics behavior under high fluence is of major importance. It is a warranty that the facility can be operated at its highest energy while preserving the optics lifetime. The question that arises is how can we estimate the optics lifetime?

In regards to the nanosecond regime, the first trend was to estimate laser damage resistance through a threshold measurement on a representative sample or a small area of the full scale part. Standardized procedures are widely used in many laboratories such as the 1/1 or S/1 tests [7]. If this approach can bring information to optimize the damage resistance of the optics, it showed up to be insufficient to predict the optics behavior on large facilities such as NIF or LMJ. In this regime, damage is mainly defects driven, and damage sites can grow dramatically under iterative shots. Consequently, optics lifetime is lowered by rare defects. To overcome this problem, rasterscan procedures were developed giving access to damage density as a function of fluence on the full scale optic [8,9].

In the nanosecond regime, laser damage in dielectric optical materials has a statistical behavior that is related to initiation on precursor defects [10–12]. The damage process is the result of complex multiphysics phenomena involving absorption, heating, material phase changes, hydrodynamics process, and plasma formation. Because nanosecond pulses are relatively long in duration compared to the timescales of these processes, small precursors can initiate a cascade of events that can result in a macroscopic damage [13]. On the contrary, damage in the sub-picosecond regime is basically driven by multiphotonic absorption. Other phenomena cannot assist the energy deposition process because of the short pulse duration. Damage has therefore a strong nonlinear dependence on intensity [14], and no statistical variations in the initiation of the damage process are expected [15]. This deterministic effect pushed people to use 1/1 or S/1 threshold measurements to estimate optics laser damage performances in the sub-picosecond regime [16–19]. Consequently, the potential role of localized defects was neglected.

The questions we have tried to answer in the present report are: Is threshold, as defined by 1/1 or S/1 tests, a good indicator of the full scale optics behavior in short pulse regime? Are there localized defects reducing drastically the fluence that can be withstood by the optics?

To address these two questions, we analyze the behavior of three high-reflective (HR) mirrors under sub-picosecond irradiations. All three mirrors are HfO_2/SiO_2 HR coatings with a SiO_2 overcoat operating at 1053 nm. Mirror 1 {design: [Glass: (HL)^15 H 2L: Air]} is manufactured using an e-beam deposition process with ion beam assistance. Mirror 2 {design: [Glass: (HL)^17 H 2L: Air]} is manufactured using an e-beam deposition process. Both samples are optimized for p-polarization and a 45° incidence. Mirror 3 {design: [Glass: (HL)^11 H 2L: Air]} is manufactured using an e-beam deposition process. It is

optimized for *s*-polarization and 40° incidence. All mirrors are tested in their operating conditions. Samples were stored in low outgassing PETG boxes. The initial contamination of samples as well as the impact of higher levels of organic contamination on the laser-induced damage threshold (LIDT) in the sub-picosecond regime has been investigated elsewhere [20]: we evidenced that the impact of organic contamination was negligible on threshold.

The laser-induced damage study of these three samples was conducted in a laser test facility called DERIC at CEA CESTA. It uses a S-pulse Amplitude Systèmes Laser source, which delivers 2-mJ pulses at 1053 nm. It operates at 10 Hz and the pulse duration, estimated from the measurement of a recurrent autocorrelator, is 675 fs. In the sample plane, the Gaussian shaped focused spot has a 155-μm diameter at $1/e$. Its measurement is realized for each pulse in a sampling path, at a plan optically equivalent to that of the sample. At the same time, an energy measurement is performed in a sampling path calibrated with respect to the energy on the sample. Both lead to the knowledge of the absolute fluence values for each laser shot on the front side of the component. For a set value, shot-to-shot fluctuations are weak: a standard deviation of 2% on fluences is typically measured. Taking into account the error margin of each instrument, fluence is given with an accuracy better than 10%. Damage detection is achieved by means of a differential interference contrast (DIC) microscope with a 100× magnification, in accordance with the ISO standard [7].

First, 1/1 and S/1 tests are performed in order to determine the LIDT of the three samples. 10 sites are fired per fluence. The results of 1/1 tests, presented in Fig. 1, show the deterministic damage behavior in this regime caused by nonlinear absorption, as discussed previously, except for Mirror 3 for which damage events can occasionally occur when tested sites are irradiated at a fluence lower than 3.4 J/cm^2. For this mirror, DIC microscopy

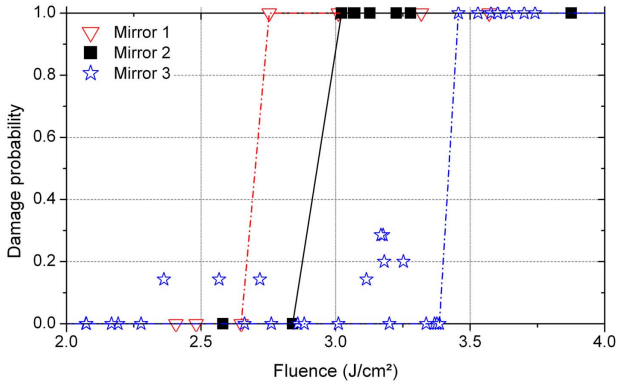

Fig. 1. Results of the 1/1 tests of the three HR coatings. Damage probabilities are represented as function of normal beam fluences. Damage behavior intrinsic to the material is under investigation. Mirrors 1 and 2, tested in the same operating conditions (incidence 45° and *p*-polarization), have a 1/1 LIDT of 2.74 J/cm^2 and 2.93 J/cm^2, respectively. Mirror 3 (operating conditions: 40° incidence, *s*-polarization) has a 1/1 LIDT of 3.41 J/cm^2. Guides for the eyes show the deterministic evolution of damage probabilities.

observations reveal morphological differences between damage sites initiated at fluences lower and higher than this value, as shown in Fig. 2: they are small and localized for fluences lower than 3.4 J/cm^2, whereas large structuration of the top layer appears for fluences higher than 3.4 J/cm^2.

For the two other mirrors, damage events during 1/1 tests arising for a fluence slightly higher than 1/1 LIDT consist of a periodic structuration of the top layer. These morphologies are usually referred to as laser-induced periodic surface structures (LIPSS) [21]. They occur upon excitation of materials at the onset of damage threshold as a consequence of complex mechanisms that will not be treated here. For higher fluences, damage sites exhibit a central area where the top layer is delaminated, surrounded by LIPSS. DIC microscopy observations of these two kinds of damage sites are reported in Fig. 3, and are similar to damage morphologies presented in Fig. 2(b). Considering only these morphologies as damage manifestation intrinsic to coating materials, 1/1 LIDT of Mirror 3 can be refined, as shown with the guide for eyes in Fig. 1. S/1 tests results are presented in Table 1 and show the so-known incubation effect [22], stemmed by an accumulation of electronic defects after several irradiation.

Simulation of the electric-field distribution realized with the TFCalc software [23] emphasizes a strong enhancement in the top layer, which is consistent with its delamination. Thereby, 1/1 and S/1 procedures in the sub-picosecond regime permit to assess damage thresholds, intrinsic to the structure and the materials, up to now used to discriminated which mirror is the best.

Second, rasterscan tests are carried out on the mirrors. They consist of scanning an area at a constant fluence to increase the number of tested sites. The sample, put on

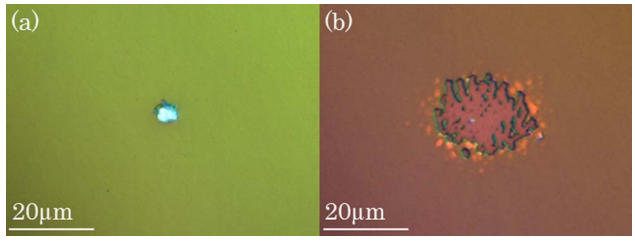

Fig. 2. DIC micrographs of damage sites initiated during 1/1 tests on Mirror 3 at 3.16 J/cm^2 (a) and 3.56 J/cm^2 (b).

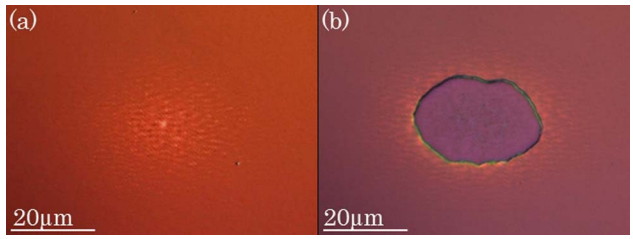

Fig. 3. DIC micrographs of typical damage sites obtained during 1/1 tests on Mirror 2. The same morphologies have been observed on Mirror 1. Fluences of test are 3.06 J/cm^2 (a) and 3.14 J/cm^2 (b). Slightly above damage threshold, LIPSS are observed. For higher fluences, delamination occurs, but damage sites are still surrounded by LIPSS.

Table 1. Results of S/1 Tests: Measured LIDT of the HR Coatings as Function of the Number of Irradiations

	LIDT (J/cm^2)		
	1/1	10/1	100/1
Mirror 1	2.74	2.61	2.54
Mirror 2	2.93	2.78	2.50
Mirror 3	3.41	3.32	3.27

motorized stages, is translated along one direction while being irradiated by the laser at a rate of 10 Hz. Since the beam spatial profile is Gaussian and in order to irradiate the largest fraction of the area homogeneously, scans are realized with a step shot-to-shot smaller than beam diameter, inducing a beam overlap here chosen to be about 80%. When only few shots are fired during 1/1 tests (10 shots per fluence), thousands of shots are fired during rasterscan (about 3200 shots), thus drastically increasing the irradiated area with respect to classical tests procedures. Only one scan is performed on each area, meaning that each site is irradiated only once. Rasterscan tests are performed at fluences lower than the 100/1 LIDT on each mirror. Moreover, because of the small beam overlap, damage events cannot be related to incubation effect. Usually applied in the nanosecond regime [9], the aim of this procedure is to reveal all defects that could trigger damage. Hence, we made various rasterscans on 5 mm $*$ 5 mm areas on the samples, at different predetermined control fluences. Results of these tests are given in terms of damage density, here calculated as the ratio between the number of damaging events and the scanned area. For each fluence, several areas are scanned to increase the statistic but also to check the homogeneity of the sample. An *in situ* damage detection technique, using a continuous probe laser beam, has been put in place. It is based on the evolution of the tested sites surface diffusion during irradiation: the probe beam is scattered when damage occurs. This damage detection system has already been described elsewhere [24] except that it works in transmission in our case. DIC microscope observations performed after rasterscan revealed that the smallest detected damage is about 4 μm.

All three mirrors are tested using this rasterscan procedure. Results are presented in Fig. 4. The main information given by these tests is that damage events occur even for fluences lower than the 1/1 LIDT. Damage sites appear for fluences as low as 20% of the 1/1 LIDT. Moreover, damage densities increase with the fluence for all three mirrors with different slopes. Considering the range of damage densities measured [5–50 dam/cm^2], the sizes of the scanned areas are well adapted: for damage densities lower than 1 dam/cm^2, a larger surface has to be scanned in order to increase the probability of damage to occur.

For each component, damage sites are uniformly distributed on a scanned area, and no propagation effect of the damage occurred. Observations of these damage sites have been carried out using both a DIC microscope and a scanning electron microscope (SEM). In Fig. 5(a), four typical damage morphologies are observed. Due to

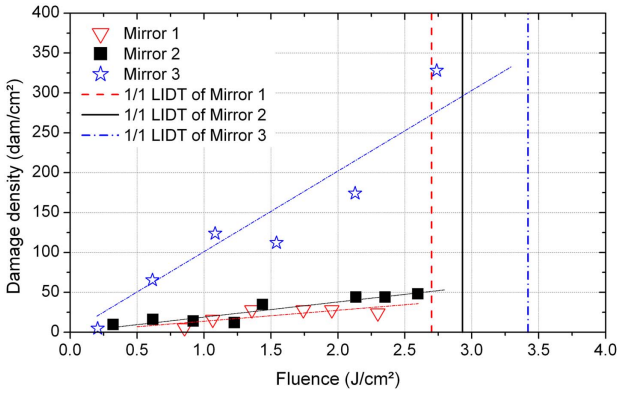

Fig. 4. Damage densities versus fluence. The damage density is calculated as the ratio between the number of damaging events detected during a scan at a set fluence and the scanned area. For all three mirrors, damage appears down to 20% below the 1/1 threshold. Moreover, damage density increases with fluence. Lines are guides for the eyes.

their proximity, we assume that they have been irradiated by the same laser shot, at the same fluence. Contrary to damage sites presented in Fig. 3, no LIPSS appear. It confirms that these damage sites revealed by rasterscans and similar to that reported in Fig. 2(a) cannot be related to the intrinsic behavior of the material. Damage events on Mirror 3 during 1/1 tests for fluences lower than the intrinsic LIDT of the coating are thus consistent with the high damage densities measured on this mirror. Figure 5 evidences nodule ejections, embedded in

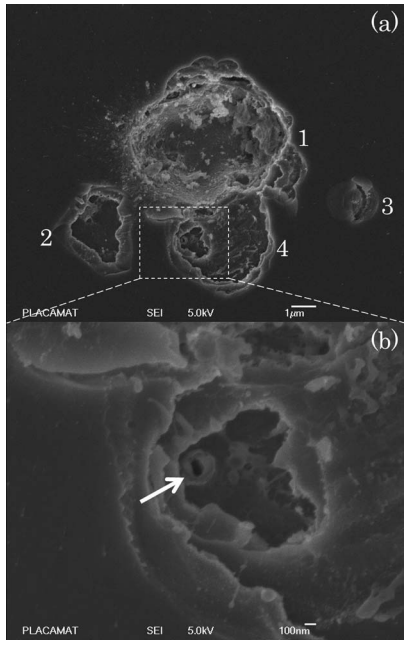

Fig. 5. SEM observation of nodules-induced damage with increasing scales. (a) This site has been irradiated by only one pulse. Four ejections are observed, noted 1, 2, 3, and 4. Ejection 1 is the strongest: all layers have been removed with extended damage. On ejection 2, few layers have been delaminated. Ejection 3 is smoother: the top layer is still partially attached to the coating. On ejection 4, a zoom on the damaged area (b) shows the location of the initiator nodule, pointed by an arrow.

the HR stack during the coating with delamination of the top layers. A location of an initiator nodule with a size around 100 nm is seen in Fig. 5(b). Here, damage sites ejections present a large variety of morphologies. Recently, Gallais *et al.* [25] studied the strong enhancement of the electric field caused by silica microspheres of one determined size embedded in HR coatings. They showed a strong correlation between electric-field enhancement induced by the defects and the LIDT in the sub-picosecond regime, and they observed one typical damage morphology. Concerning our HR coatings, the random distribution of defects, possible cooperative effects between them added to a likelihood of different populations of defects (size, nature, depth in the coating) [26], contribute to electric-field enhancements with different amplitudes and thus, potential differences in the morphologies. The established models are commonly 1D models and concern the interaction of ultra-short pulse with a material considered perfect or presenting electronic defects. With respect to the presented results, the role of spatially localized defects must be added to 3D calculation method taking into account their geometry and their nature to predict the laser resistance of a coating.

These experimental results demonstrate that defects catastrophically reduce the damage resistance of a coating. LIDT in the sub-picosecond regime is classically governed by the material properties (energy bandgap and refractive index) [27] and the enhancement of the electric-field in the HR structure [18], but defects embedded in coatings can strongly modify the electric-field distribution. Damage densities are measured even for low fluences of irradiation on all three mirrors, but their evolutions with the fluence are different. Using Fig. 1, a first assessment of the damage resistance of these optical components can be done, but their full scale performances are questionable considering rasterscans results: Mirror 3, which has a 1/1 LIDT 20% higher than Mirror 1, exhibits damage densities 10 times higher. Moreover, Fig. 4 shows that there is no correlation between 1/1 and rasterscan tests results. On the basis of this study, we demonstrate that damage density is a parameter that must be taken into account for the characterization of an optical component when a precise knowledge of its behavior under high power is sought. It brings a new viewpoint for the optimization of manufacturing processes of coatings for the sub-picosecond regime, and also may lead to a better prediction of the optics lifetime in operating condition, which means after irradiations by large beam.

This work is partially supported by the Conseil Régional d'Aquitaine, through the ENDOPICO project (Contract No. 20 131 603 005). We would like to acknowledge Philippe Legros (PLACAMAT, UMS 3626) for SEM observations.

References

1. G. Verlarde and N. C. Santamaria, *Inertial Confinement Nuclear Fusion: A Historical Approach by Its Pioneers* (Foxwell & Davies, 2007).
2. F. Floux, D. Cognard, L.-G. Denoeud, G. Piar, D. Parisot, J. Bobin, F. Delobeau, and C. Fauquignon, Phys. Rev. A **1**, 821 (1970).
3. M. L. Andre, Fusion Eng. Des. **44**, 43 (1999).
4. G. H. Miller, E. I. Moses, and C. R. Wuest, Opt. Eng. **43**, 2841 (2004).
5. D. Strickland and G. Mourou, Opt. Commun. **56**, 219 (1985).
6. J. Zuegel, S. Borneis, C. Barty, B. Legarrec, C. Danson, N. Miyanaga, P. Rambo, C. Leblanc, T. Kessler, A. W. Schmid, L. Waxer, J. H. Kelly, B. Kruschwitz, R. Jungquist, E. Moses, J. Britten, I. Jovanovic, J. Dawson, and N. Blanchot, Fusion. Sci. Technol. **49**, 453 (2006).
7. ISO Standard Nos. 21254-1–21254-4 (2011).
8. L. Sheehan, S. Schwartz, C. Battersby, R. Dickson, R. Jennings, J. Kimmons, M. Kozlowski, S. Maricle, R. Mouser, M. Runkel, and C. Weinzapfel, Proc. SPIE **3578**, 302 (1999).
9. L. Lamaignère, S. Bouillet, R. Courchinoux, T. Donval, M. Josse, J. C. Poncetta, and H. Bercegol, Rev. Sci. Instrum. **78**, 103105 (2007).
10. N. Bloembergen, Appl. Opt. **12**, 661 (1973).
11. C. W. Carr, H. B. Radousky, A. M. Rubenchik, M. D. Feit, and S. G. Demos, Phys. Rev. Lett. **92**, 087401 (2004).
12. J.-Y. Natoli, L. Gallais, H. Akhouayri, and C. Amra, Appl. Opt. **41**, 3156 (2002).
13. G. Duchateau, M. D. Feit, and S. G. Demos, J. Appl. Phys. **111**, 093106 (2012).
14. B. C. Stuart, M. D. Feit, S. Herman, A. M. Rubenchik, B. W. Shore, and M. D. Perry, Phys. Rev. B **53**, 1749 (1996).
15. A. P. Joglekar, H. Liu, G. J. Spooner, E. Meyhofer, G. Mourou, and A. J. Hunt, Appl. Phys. B **77**, 25 (2003).
16. M. D. Perry, R. D. Boyd, J. A. Britten, D. Decker, B. W. Shore, C. Shannon, and E. Shults, Opt. Lett. **20**, 940 (1995).
17. T. Clausnitzer, J. Limpert, K. Zollner, H. J. Fuchs, E. B. Kley, A. Tunnermann, M. Jupe, and D. Ristau, Appl. Opt. **42**, 6934 (2003).
18. J. Néauport, E. Lavastre, G. Razé, G. Dupuy, N. Bonod, M. Balas, G. de Villele, J. Flamand, S. Kaladgew, and F. Desserouer, Opt. Express **15**, 12508 (2007).
19. J. Qiao, A. W. Schmid, L. Waxer, T. Nguyen, J. Bunkenburg, C. Kingsley, A. Kozlov, and D. Weiner, Opt. Express **18**, 10423 (2010).
20. O. Favrat, M. Sozet, I. Tovena-Pécault, L. Lamaignère, and J. Néauport, Proc. SPIE **9237**, 923707 (2014).
21. J. Z. P. Skolski, G. R. B. E. Römer, J. Vincenc Obona, and A. J. Huis in't Veld, J. Appl. Phys. **115**, 103102 (2014).
22. M. Mero, B. Clapp, J. C. Jasapara, W. Rudolph, D. Ristau, K. Starke, J. Krüger, S. Martin, and W. Kautek, Opt. Eng. **44**(5), 051107 (2005).
23. TFCalc software, http://www.sspectra.com/.
24. L. Lamaignère, M. Balas, R. Courchinoux, T. Donval, J. C. Poncetta, S. Reyné, B. Bertussi, and H. Bercegol, J. Appl. Phys. **107**, 023105 (2010).
25. L. Gallais, X. Cheng, and Z. Wang, Opt. Lett. **39**, 1545 (2014).
26. C. J. Stolz, R. J. Tench, M. R. Kozlowski, and A. Fornier, Proc. SPIE **2714**, 374 (1996).
27. M. Mero, J. Liu, W. Rudolph, D. Ristau, and K. Starke, Phys. Rev. B **71**, 115109 (2005).